

# T1 Signal Hyperintensity in the Sellar Region: Spectrum of Findings<sup>1</sup>

## CME FEATURE

See accompanying test at [http://www.rsna.org/education/rg\\_cme.html](http://www.rsna.org/education/rg_cme.html)

## LEARNING OBJECTIVES FOR TEST 4

After reading this article and taking the test, the reader will be able to:

- Recognize normal entities with T1 hyperintensity in the sellar region.
- Identify sellar and parasellar lesions that exhibit high T1 signal intensity.
- Describe the specific sources of T1 hyperintensity after surgery or medical therapy.

## TEACHING POINTS

See last page

*Fabrice Bonneville, MD • Françoise Cattin, MD • Kathlyn Marsot-Dupuch, MD • Didier Dormont, MD • Jean-François Bonneville, MD • Jacques Chiras, MD*

T1 signal hyperintensity is a common finding at magnetic resonance imaging of the sellar region. However, this signal intensity pattern has different sources, and its significance depends on the clinical context. Normal variations in sellar T1 signal hyperintensity are related to vasopressin storage in the neurohypophysis, the presence of bone marrow in normal and variant anatomic structures, hyperactive hormone secretion in the anterior pituitary lobe (eg, in newborns and pregnant or lactating women), and flow artifacts and magnetic susceptibility effects. Pathologic variations in T1 signal hyperintensity may be related to clotting of blood (in hemorrhagic pituitary adenoma, pituitary apoplexy, Sheehan syndrome, or thrombosed aneurysm) or the presence of a high concentration of protein (Rathke cleft cyst, craniopharyngioma, or mucocoele), fat (lipoma, dermoid cyst, lipomatous meningioma), calcification (craniopharyngioma, chondroma, chordoma), or a paramagnetic substance (manganese, melanin). After treatment, T1 signal hyperintensity may result from the presence of materials used for surgical packing (gelatin sponge, fat); from compression of the cavernous sinus and reduction of the venous flow, caused by overpacking of the operative bed; or from hormone hypersecretion by a remnant of normal tissue in the anterior lobe of the pituitary gland.

©RSNA, 2006

An earlier incorrect version of this article appeared online and in print. This article was corrected on September 24, 2021.

RadioGraphics 2006; 26:93–113 • Published online 10.1148/rg.261055045 • Content Codes: **MR** **NR**

<sup>1</sup>From the Department of Neuroradiology, Pitié-Salpêtrière Hospital, 74 Boulevard de l'Hôpital, 75013 Paris, France (F.B., D.D., J.C.); Department of Neuroradiology, Jean Minjot Hospital, Besançon, France (F.C., J.F.B.); and Department of Neuroradiology, Bicêtre Hospital, Le Kremlin-Bicêtre, France (K.M.). Recipient of an Excellence in Design award for an education exhibit at the 2004 RSNA Annual Meeting. Received March 7, 2005; revision requested April 12 and received May 4; accepted May 5. All authors have no financial relationships to disclose. Address correspondence to F.B. (e-mail: [fabrice.bonneville@psl.ap-hop-paris.fr](mailto:fabrice.bonneville@psl.ap-hop-paris.fr)).

©RSNA, 2006

**Table 1**  
**Normal Causes of T1 Signal Hyperintensity**

Structure	Source of T1 Signal Hyperintensity	Appearance on T1-weighted Images	Comments
Pituitary gland			
Posterior lobe	Vasopressin storage	Focus of high T1 signal intensity located immediately anterior to the dorsum sellae	T1 signal hyperintensity is function-related and may be ectopic in dwarfism
Anterior lobe	Hormonal hypersecretion	Mild homogeneous hyperintense T1 signal of the adenohypophysis	Observed in newborns and pregnant or lactating women
Bone	Marrow fat	High T1 signal intensity in parasellar nonpneumatized bone structures (eg, sphenoid body, clinoid processes, dorsum sellae)	Large sellar spine may contain marrow fat
Sellar floor	Magnetic susceptibility effect	Small focus of hyperintense signal	Amplified by the use of gradient-echo sequences
Arteries	Flow artifact	Small focus of hyperintense signal	Amplified by the use of gradient-echo sequences

### Introduction

T1 signal hyperintensity in and near the sella turcica has interested radiologists since the introduction of magnetic resonance (MR) imaging in the 1980s. The “bright spot” in the posterior lobe of the pituitary gland was among the earliest noted and most passionately debated examples of this finding on MR images (1–6). Initially thought to indicate a fat pad (1), the finding was quickly established as a normal representation of the functional storage of vasopressin in the posterior pituitary lobe (4,5,7,8). A voluminous literature rife with controversy demonstrates radiologists’ fascination with intrinsic T1 signal hyperintensity. This article surveys the possible sources of this signal intensity pattern in the sellar region. The sellar region is centered around the adenohypophysis, which is described in the literature as isointense both to the pons on sagittal T1-weighted images and to the white matter of the temporal lobes on coronal T1-weighted images (2,7,9). With the pituitary gland used as an anatomic reference, two sources of high T1 signal intensity may be defined in the sellar region:

(a) the adenohypophysis itself, if its signal intensity is homogeneously higher than that of either the pons or the white matter of the temporal lobe, and (b) any structure showing a signal intensity higher than that of the normal anterior pituitary lobe.

T1 signal hyperintensity on MR images is due to the T1-shortening effect of the object imaged. A short T1 produces high signal intensity on spin-echo images obtained with relatively short relaxation time and echo time, because the 180° pulse interrogates the imaging volume before T2 relaxation has occurred and, thus, the T1 effects of the 90° pulse are magnified. In other words, because of the short relaxation time, saturation has not occurred and T1 differences are emphasized. In normal sellar structures, as in other parts of the human anatomy, T1 signal hyperintensity may be due to a high intracellular protein content (from hormone hypersecretion in the anterior pituitary lobe or from vasopressin storage in the posterior pituitary lobe), lipids (bone marrow), deposition of paramagnetic substances (manganese), or artifacts (magnetic susceptibility, slow flow). In sellar or parasellar lesions, a short T1 may be related to the presence of intra- or extracellular methemoglobin or a cyst with a high concentration of protein, fat, and/or calcification.



**Figure 1.** Normal T1 signal hyperintensity of the posterior pituitary lobe in a young healthy volunteer. Axial T1-weighted MR image clearly depicts a bright spot in a depression slightly lateral to the midline (long arrow), immediately anterior to the thin linear area of signal hypointensity in the anterior cortex of the dorsum sellae (arrowhead). Note the asymmetric appearance of the marrow fat within the dorsum sellae (short arrow) and the irregular but normal margins of the posterior lobe.

To assist radiologists in recognizing the different possible sources of T1 signal hyperintensity in the sellar and parasellar areas, this article provides an overview of such findings grouped according to their origins: (a) variable normal conditions (eg, in newborns and pregnant or lactating women), (b) lesions in or near the sella turcica, or (c) post-therapeutic conditions.

### Variable Normal Conditions

The possible normal causes of T1 signal hyperintensity are listed, and their MR appearances are described, in Table 1.

### Vasopressin Storage

A focal spot of hyperintense T1 signal is usually observed at the posterior aspect of the sella turcica, immediately anterior to the dorsum sellae. The finding has a unique cause: It has been demonstrated conclusively to result specifically from the storage of vasopressin (3), a hormone synthesized by the hypothalamus and normally stored in the posterior pituitary lobe. To enable its descent

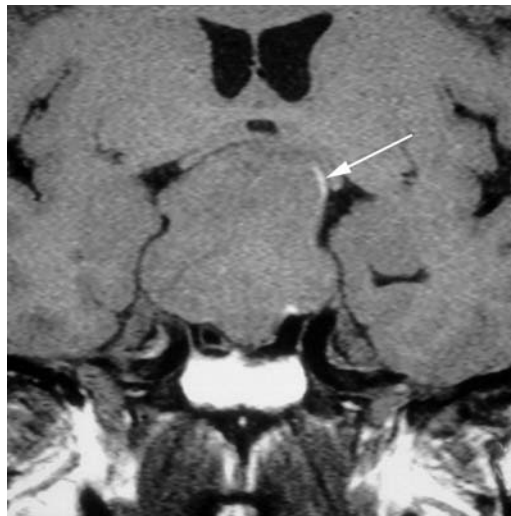


**Figure 2.** Giant macroadenoma in a 65-year-old man with bitemporal superior quadrantanopia. Coronal T1-weighted image depicts an ectopic but functional location of vasopressin storage, displaced from the midline, at the dome of the lesion (arrow).

through the hypothalamic axons to the posterior lobe, this hormone is bound to a macroprotein structure, the so-called vasopressin-neurophysin II-copeptin complex, which shortens the T1 signal (8). **The resultant focal spot of high signal intensity on MR images correlates with normal function and is observed where the vasopressin is stored, normally in the posterior pituitary lobe,** which is located in a small depression in the dorsum sellae and is almost always depicted at dedicated thin-section axial T1-weighted imaging in normal young volunteers (Fig 1) (10,11). **A focus of high signal intensity also may be observed outside the sella in individuals in whom the hypothalamohypophyseal axis is interrupted or extrinsically compressed (12).** For example, in those with hypophysial dwarfism, the location of normal vasopressin storage is visualized as a high-signal-intensity focus at the distal tip of a sectioned stalk (13). The focal area of high signal intensity also may be seen at an obstructed infundibulum, or anywhere along the surface of a macroadenoma with a height of more than 20 mm (Fig 2) (11,14), but it is not seen in patients with central diabetes insipidus (3).

**Teaching Point**

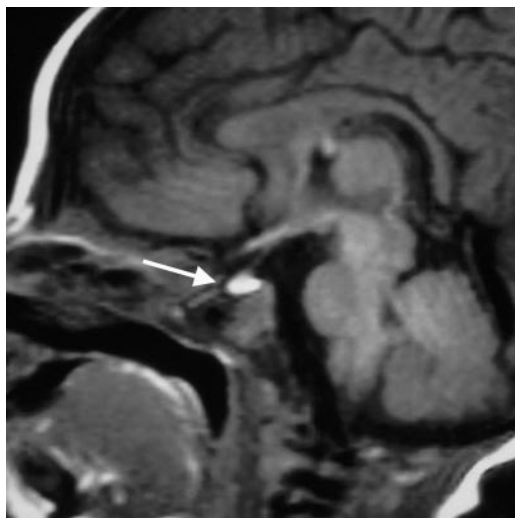


**Figure 3.** Normal MR signal intensity pattern of the sellar region in a 3-week-old newborn examined for hypotonia. Sagittal T1-weighted image shows the homogeneous and marked signal hyperintensity of the adenohypophysis that is usually observed at this age (arrow).

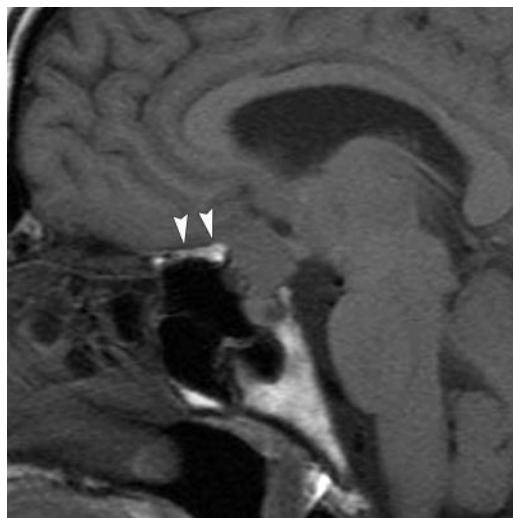


**Figure 4.** Meningioma of the tuberculum sellae in a 33-year-old woman. Sagittal T1-weighted image depicts the common hyperostotic reaction adjacent to the tumor, which, in this patient, is located at the planum sphenoidale (arrowheads). The thickened bone contains fatty marrow, which accounts for the T1 signal hyperintensity.

### Anterior Pituitary Lobe Hyperactivity

On T1-weighted images, the signal of the normal anterior pituitary lobe appears isointense to those of the pons on sagittal images and the temporal-lobe white matter on coronal images. **Various normal physiologic circumstances may produce anterior pituitary lobe hyperactivity in the form of cellular hormonal hypersecretion, which results in an increase in the intracellular protein concentration and, therefore, a shortening of T1. These circumstances include the first few weeks of life for newborns (Fig 3) and, for women, pregnancy, the postpartum period, and lactation (15–17).**

Teaching  
Point

### Bone

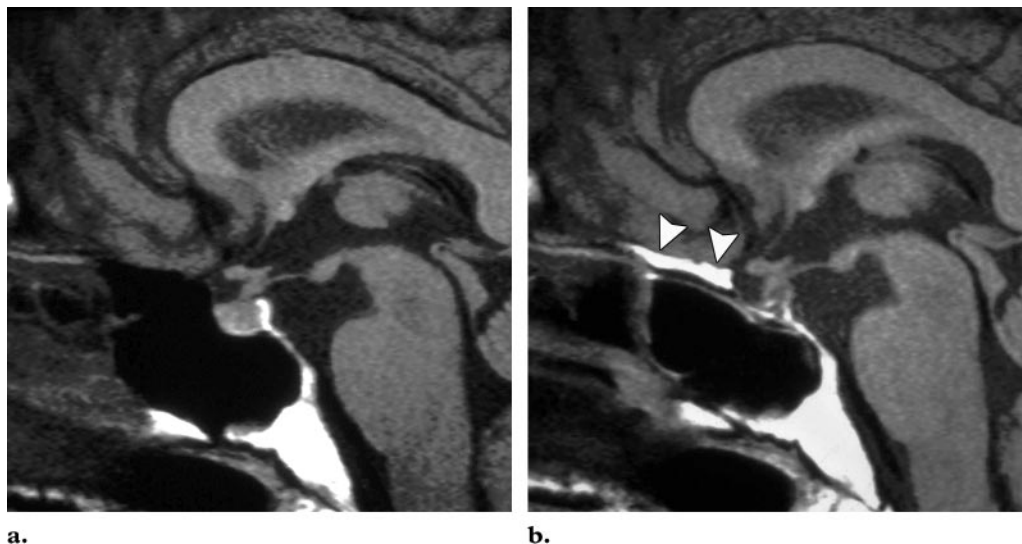
In normal subjects, the bone marrow is fatty and is depicted with homogeneous high signal intensity on T1-weighted MR images. In most individuals, the dynamic phenomenon of pneumatization extends deeply into the sphenoid body, to the embryological presphenoid–postsphenoid junction, which roughly corresponds to an imaginary vertical line through the middle of the sella turcica on sagittal MR images (18). It may also extend to the sphenoccipital synchondrosis. Thus, the posterior aspect of the sphenoid body, the dorsum sellae, and the posterior clinoid processes are usually hyperintense, whereas the ante-



**Figure 5.** Juvenile angiofibroma in an 18-year-old man with epistaxis and nasal obstruction. Sagittal T1-weighted image depicts a mass that fills the sphenoid sinus, with a classic vascular pattern that includes numerous serpentine flow voids (arrowheads). Note the unusual hyperostotic reaction of the planum sphenoidale, which outlines the upper aspect of the mass (arrow), and the signal intensity pattern of normal red bone marrow in the clivus and C2 vertebra.

rior part of the sphenoid body is completely pneumatized and void of signal. However, a few exceptions, possibly caused by a phenomenon similar





**a.** **b.**  
**Figure 6.** Microadenoma in a 37-year-old woman with hyperprolactinemia. Sagittal T1-weighted images acquired before (**a**) and 12 months after (**b**) surgery with a transsphenoidal approach show a postoperative increase in signal intensity in the jugum (arrowheads), a finding that is related to bone remodeling after surgery.

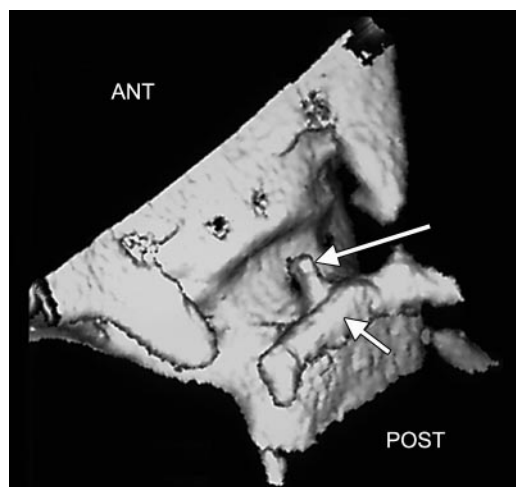


**Figure 7.** Incidental finding of a sellar spine in a 17-year-old male patient with head trauma. Three-dimensional reformatted head computed tomographic (CT) image depicts a midline spur (long arrow) anterior to the dorsum sellae (short arrow).

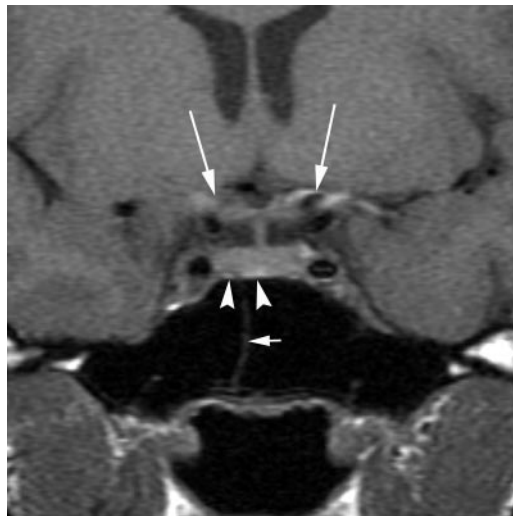
A rare variant in bone structure, referred to as sellar spine, also may appear hyperintense on T1-weighted MR images. The variant involves a midline spur that projects anteriorly from the dorsum sellae and that is thought to correspond to a remnant of the most cranial aspect of the notochord (Fig 7) (20). If the spur is large enough, it may contain bone marrow and, therefore, may include a region with T1 signal hyperintensity (21).

to hyperostosis frontalis interna, may be observed in healthy elderly people and in individuals with certain pathologic conditions. Abnormality of the planum sphenoidale or the underlying sphenoid mucosa may lead to thickening and ossification of the jugum, in which case the jugum exhibits high signal intensity on T1-weighted MR images, a distinctive finding. This subtle sign is visible in skull-base meningioma (Fig 4) and in various slow-growing tumors of the sinuses (eg, juvenile nasopharyngeal angiofibroma [Fig 5]). It is rarely seen in pituitary adenoma, except after surgery with a transsphenoidal approach (Fig 6) (19).

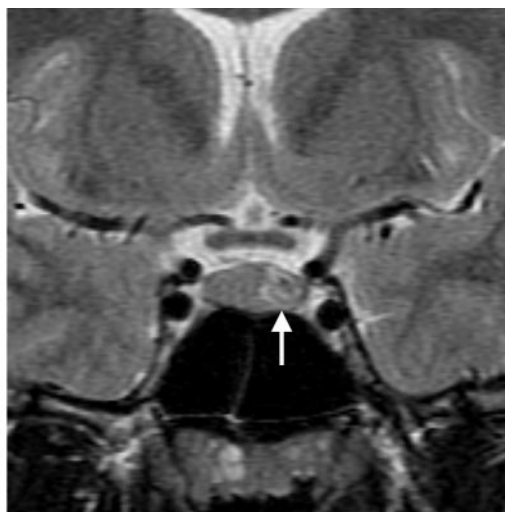
## Artifacts

**Magnetic Susceptibility Effect.**—The pneumatized sphenoid body is separated from the sella by the cortical bone of the sellar floor. The abrupt transition between air-filled bone and dense cortical bone results in distortion of the local magnetic field, which, on T1-weighted and other MR images, produces a subtle increase in signal intensity

**Figure 8.** Coronal T1-weighted image in a 25-year-old woman with mild hyperprolactinemia shows a subtle magnetic susceptibility effect at the sphenoid sinus–sellar floor interface (arrowheads), which is interrupted by the bony nasal septum (short arrow), and high-signal-intensity flow artifacts in the arteries of the circle of Willis (long arrows).



**a.**



**b.**

**Figure 9.** Silent hemorrhagic pituitary adenoma in a 32-year-old woman with hyperprolactinemia. Coronal T1-weighted image (**a**) and T2-weighted image (**b**) show a pituitary microadenoma with a lateral location in the left part of the gland. The heterogeneous circumferential signal intensity on the T2-weighted image is highly suggestive of bleeding (arrow).

in the pituitary gland, just above the small convexities of the sellar floor (Fig 8). This is why gradient-echo sequences, which are exquisitely sensitive to local magnetic field alterations and therefore amplify this artifact, should be used with caution during imaging of the sellar area (7).

**Flow Artifact.**—Because the arteries of the circle of Willis surround the sella turcica, flow artifacts may be observed in this region. Paradoxical enhancement and entry section phenomena may produce areas of T1 signal hyperintensity in the arteries that are oriented in the phase-encoding direction (Fig 8) (22).

### Lesions in or Near the Sella Turcica

The lesions that may have T1 signal hyperintensity on MR images are listed and described in Table 2.

#### Blood Clots and Hemorrhages

The MR imaging features of clots and hemorrhagic lesions evolve in accordance with the presence of various products of the breakdown of hemoglobin. T1 signal hyperintensity may correspond to intracellular and extracellular methemoglobin. It may also be seen during the chronic stage of a clot or hemorrhage, when sedimentation of the blood cells produces a distinctive fluid-debris level within the lesion.

**Table 2**  
**Lesions that Cause T1 Signal Hyperintensity**

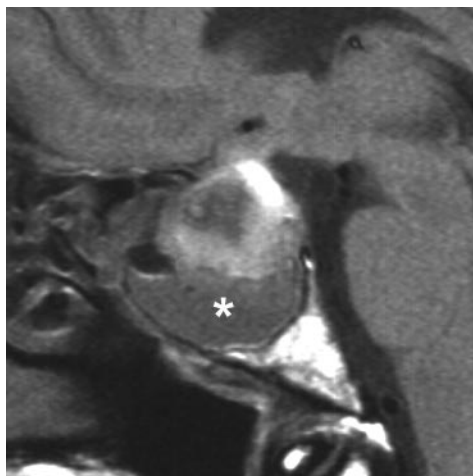
Lesion Type	Source of T1 Signal Hyperintensity	Appearance of T1 Signal Hyperintensity	Appearance on T2-weighted Images	Enhancement	Suggestive Features
Pituitary apoplexy, Sheehan syndrome	Blood	Subtle in the very acute phase	Heterogeneous	Thin peripheral rim	Thickening of the sphenoidal mucosa; hyperintense signal on diffusion-weighted images
Chronic hemorrhagic adenoma	Blood	Fluid-fluid level	Fluid-fluid level	Mild	Figure-of-eight shape; enlargement of the sella
Aneurysm	Blood	Heterogeneous	Heterogeneous	When present, heterogeneous	Contact with an artery; remodeling of bone
Rathke cleft cyst	High protein content	Homogeneous (variable); no fluid-fluid level	Hypointense (variable)	None	Possible intracystic micronodule, best seen on T2-weighted images
Craniopharyngioma	Multiple*	Heterogeneous	Heterogeneous	Thick peripheral rim and/or nodular	Solid, calcified, and cystic components; suprasellar location
Chordoma	Multiple*	Variable	Hyperintense	Heterogeneous	Lytic lesion of the clivus, with intratumoral septa
Chondroid tumor	Calcification	Intratumoral foci	Hyperintense	Patchy	Lateral origin from a synchondrosis
Abscess	High protein content	Subtle; mainly at the periphery	Hyperintense	Peripheral capsule	Intense local-regional inflammatory reaction
Mucocele	High protein content	Intense and homogeneous	Hyperintense	None	Erosion of the walls of the sphenoid bone
Lipoma	Fat	Intense	Intense on T2-weighted SE images	None	Exactly matches signal intensity of fat on all MR images; chemical shift
Dermoid cyst	Fat	Intense and homogeneous, except if calcification is present	Similar to that on T1-weighted images	Rarely, at the peripheral capsule	Subarachnoid droplets and fat-fluid level in the presence of a ruptured cyst
Meningioma	Multiple*	Mainly located at the osseous insertion	Iso- to hyperintense	Intense and dural tail sign	Hemispheric shape

\*T1 signal hyperintensity may vary with the combination of blood, high protein content, fat, and calcification.

**Pituitary Apoplexy.**—Pituitary apoplexy is a rare clinical syndrome that corresponds to the acute hemorrhagic or ischemic transformation of a tumor-containing or normal adenohypophysis (23). The clinical symptoms include headache, visual impairment, and ophthalmoplegia. However, bleeding is common in pituitary adenomas

and is clinically silent in most cases. Indeed, in one study, up to 20% of pituitary adenomas (both micro- and macroadenomas) showed evidence of hemorrhage on MR images (Fig 9), while only 25% of patients with MR evidence of intratumoral hemorrhage had clinical apoplexy (24).

**Figure 10.** Pituitary apoplexy in a 54-year-old man with acute headache and ophthalmoplegia. Sagittal T1-weighted (a) and T2-weighted (b) images depict a lesion with heterogeneous signal intensity inside an enlarged sella, a distinctive feature of subacute hemorrhage. Note the inflammatory reaction in the sphenoid sinus (\*).



a.



b.

### Teaching Point

Early in the course of pituitary apoplexy, MR images depict a mass lesion that has heterogeneous signal intensity, with predominant hyperintensity on T1 images and predominant hypointensity on T2-weighted images (Fig 10) (25). If a macroadenoma is present, the sella is enlarged. Diffusion-weighted imaging may be helpful in the early diagnosis of acute pituitary apoplexy, because it depicts high signal intensity due to restricted diffusion (26) from ischemic damage to the gland or from the accumulation of intracellular blood products (27). At a later stage, the sedimentation of blood products may create a fluid-debris level within the mass, a finding that is highly suggestive of hemorrhagic pituitary adenoma (Fig 11). When present, a fluid-fluid level, which is most clearly depicted on axial or sagittal images, is extremely valuable because it helps to differentiate an adenoma from a Rathke cleft cyst; in the latter condition, hemorrhage and consequent fluid-fluid level have not been described (28).

**Thickening of the mucosa of the sphenoid sinus is an MR feature suggestive of the early hours of pituitary apoplexy (29).** This MR characteristic, which is thought to correspond to venous engorgement in the region, also has been reported in Sheehan syndrome, a condition that involves necrosis of the pituitary gland during the postpartum period (30). Sheehan syndrome usually occurs in cases of complicated delivery with hemorrhage and shock. Hemorrhagic transformation may occur, and methemoglobin may be represented on MR images by subtle hyperintensity of the T1 signal. Sheehan syndrome may be suspected in a case of early postpartum pituitary apoplexy in which MR images depict a swollen and nonenhancing pituitary gland with iso- or hyperintense T1 signal and a massive local inflammatory



**Figure 11.** Hemorrhagic pituitary macroadenoma in a 43-year-old man. Sagittal T1-weighted image shows a fluid-fluid level that represents the sedimentation of blood products (arrow) in the sellar region, a finding that is observed mainly in hemorrhagic pituitary adenomas.

tory reaction, with intense enhancement of the adjacent meninges and thickening of the sphenoid sinus mucosa (30).

**Aneurysms.**—The diagnosis of aneurysms is of critical importance in an evaluation of the sellar region: The arteries in the circle of Willis, which surrounds the sella turcica, are the most frequent locations of intracranial aneurysms. A round lesion with an internal signal void on spin-echo MR images, especially on those acquired with T2 weighting, is a classic feature of an aneurysm with rapid internal blood flow. However, partially thrombosed aneurysms appear as well-demarcated round parasellar or intrasellar lesions with internal T1 hyperintensity and characteristic heterogeneous T2 hypointensity (Fig 12), findings that indicate intraaneurysmal clotting. Because a giant aneurysm with partial internal clotting may



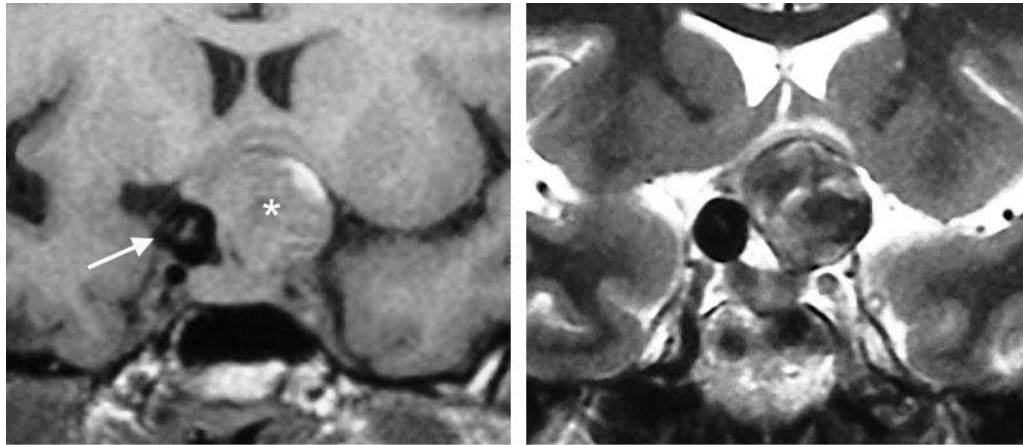


**Figure 12.** Aneurysms in the carotid and ophthalmic arteries in a 47-year-old woman with visual impairment. Coronal T1-weighted image (**a**) and T2-weighted image (**b**) show bilateral suprasellar round lesions that impinge on the optic chiasm. The heterogeneous signal intensity observed in the left-sided lesion (\* in **a**) on both images is a distinctive feature of an aneurysm with a thrombosed component, whereas the flow void in the right-sided lesion (arrow in **a**) indicates a patent aneurysm.

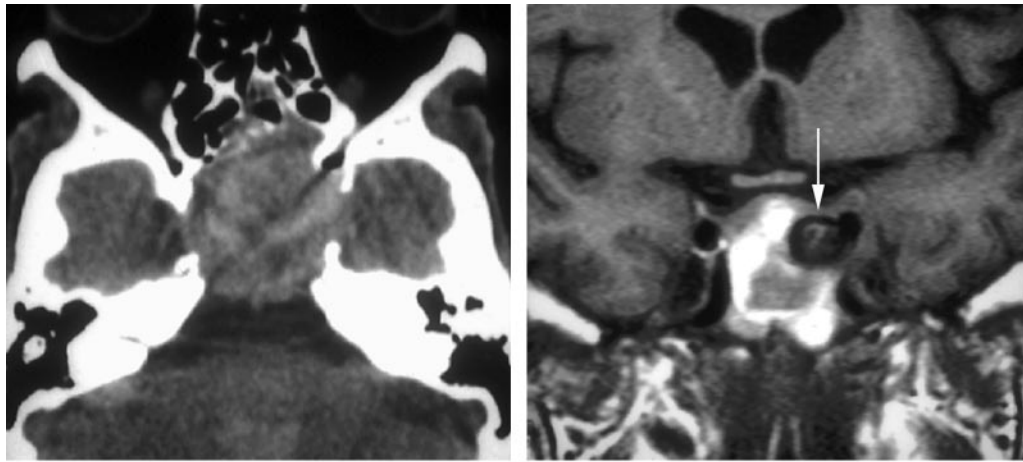
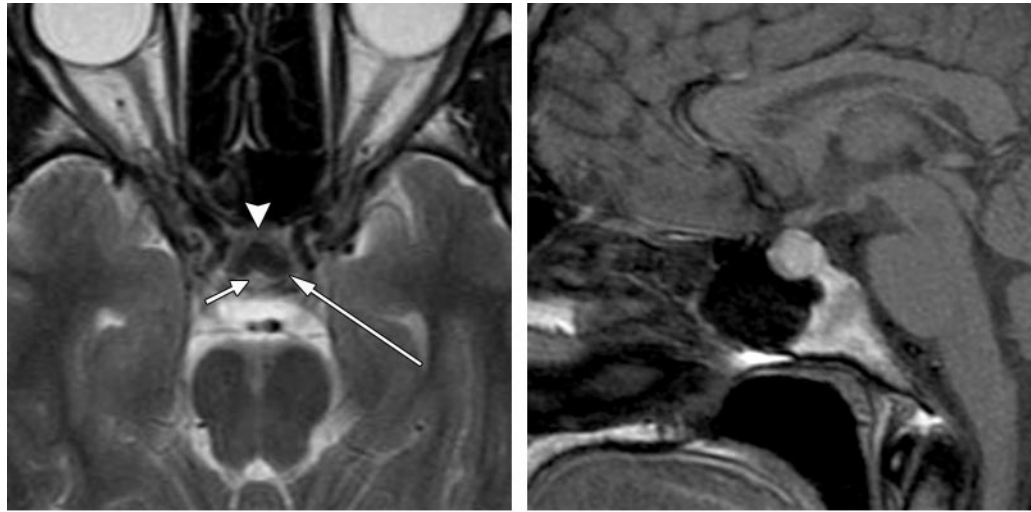


**Figure 13.** Giant partially thrombosed left carotid artery aneurysm in a 67-year-old man with headache. (**a**) Unenhanced axial CT scan reveals a giant noncalcified lesion that has destroyed the central skull base. (**b**) Coronal T1-weighted image depicts a heterogeneous lesion, with peripheral signal hyperintensity consistent with methemoglobin, in the sella turcica and the sphenoid sinus. The rounded component with no signal (arrow), adjacent to the intracavernous segment of the left internal carotid artery, is highly suggestive of residual circulation in an aneurysm, a finding confirmed by the digital subtraction angiogram (**c**).

**c.**

mimic a solid destructive tumor of the skull base (Fig 13), MR angiography or conventional angiography should be performed in cases with

these features before biopsy is considered. The finding of a residual patent lumen on images helps confirm the diagnosis of aneurysm.



**a.**  
**Figure 14.** Intrasellar Rathke cleft cyst in a 22-year-old patient with headache. **(a)** Axial T2-weighted image clearly shows the location of a kidney-shaped Rathke cleft cyst (long arrow) exactly on the imaginary midline that divides the anterior (arrowhead) and posterior (short arrow) pituitary lobes. **(b, c)** Sagittal unenhanced T1-weighted **(b)** and T2-weighted **(c)** images show a rounded homogeneous intrasellar lesion with T1 signal hyperintensity and T2 signal hypointensity (arrow in **c**). The homogeneity of the signal on images obtained with both sequences, especially on **c**, is inconsistent with a hemorrhagic lesion.



**c.**

## Lesions with High Protein Content

**Rathke Cleft Cysts.**—Rathke cleft cysts are benign cystic sellar lesions that generally are asymptomatic. The lesions are lined by a single layer of epithelial cells that derives from the Rathke pouch. At MR imaging, Rathke cleft cysts have a variable T1 signal that ranges from hypointense to hyperintense. The signal pattern depends directly on the biochemical content, especially the protein concentration (31). Cysts with a high protein content demonstrate high T1 signal intensity and usually have a low intracystic water content that leads to T2 signal decrease. **Thus, typical Rathke cleft cysts appear as nonenhancing well-demarcated intrasellar rounded lesions located exactly at the midline between the anterior and posterior pituitary lobes. The cysts have a homogeneously hyperintense T1 signal and, often, a hypointense T2 signal (Fig 14) (28).** Axial images

are crucial for identifying the specific location and characteristic kidney shape of a Rathke cleft cyst (Fig 14). Axial images also may help rule out a fluid-fluid level, a valuable capability. Indeed, the presence of a hemorrhagic fluid-debris level in an intrasellar lesion on MR images suggests a pituitary adenoma, because a Rathke cleft cyst almost never bleeds (Fig 15). However, small intracystic nodules that correspond to proteinaceous concretions may be observed in a Rathke cleft cyst (32). The nodules, which are more easily seen on T2-weighted images (Fig 16) than on T1-weighted images, have lower T2 and higher T1 signal intensity than does the rest of the cyst. In some cases, a Rathke cleft cyst may arise in the sella and extend upward beyond the confines of the sella. Finally, a cyst may have a suprasellar location, immediately above the sellar diaphragm, at

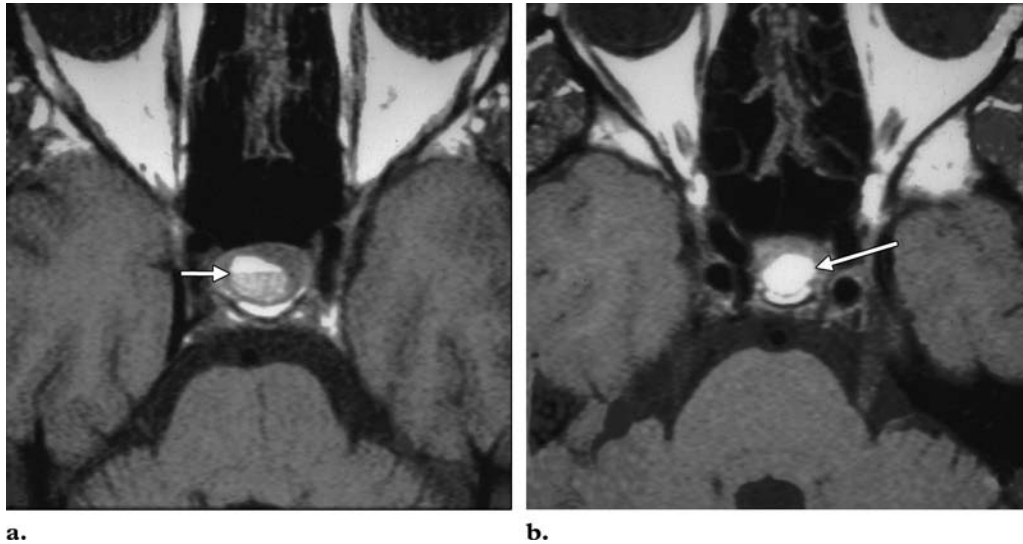


**Figure 15.** Axial T1-weighted images show a hemorrhagic pituitary microadenoma (arrow in **a**) and a Rathke cleft cyst (arrow in **b**). At initial comparison, the features of the two different lesion types may appear similar: high T1 signal intensity, rounded shape, and intrasellar location exactly on the midline between the pituitary lobes. However, the distinctive hemorrhagic fluid-debris level visible in the pituitary adenoma is absent in the Rathke cleft cyst.



**Figure 16.** Rathke cleft cyst in a 32-year-old woman with mild hyperprolactinemia. Coronal T2-weighted image shows features that are highly suggestive of a Rathke cleft cyst: tiny hypointense dots (arrowheads), which are believed to correspond to proteinaceous concretions floating inside a midline cyst.

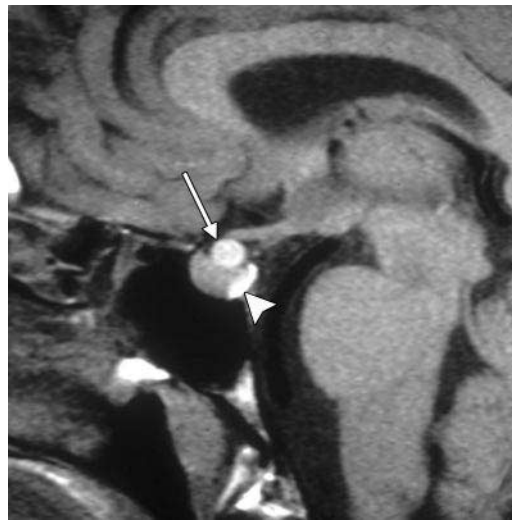


**Figure 17.** Suprasellar Rathke cleft cyst in a 28-year-old woman with mild hyperprolactinemia. Sagittal T1-weighted image shows a round and homogeneously hyperintense midline Rathke cleft cyst (arrow) in the typical suprasellar location, immediately above the sellar diaphragm and anterior to the stalk, as well as the normal area of signal hyperintensity at the posterior aspect of the sella (arrowhead).

the base of the stalk, and have identical signal intensity characteristics to those of an intrasellar Rathke cleft cyst (Fig 17) (28).

**Craniopharyngiomas.**—Craniopharyngiomas, like Rathke cleft cysts, derive from Rathke pouch cells. They usually are manifested during childhood or during the 4th or 5th decade of life by

visual symptoms or endocrine disturbances such as diabetes insipidus. They typically appear as intrasellar or suprasellar heterogeneously enhancing lesions with a tripartite structure of solid,



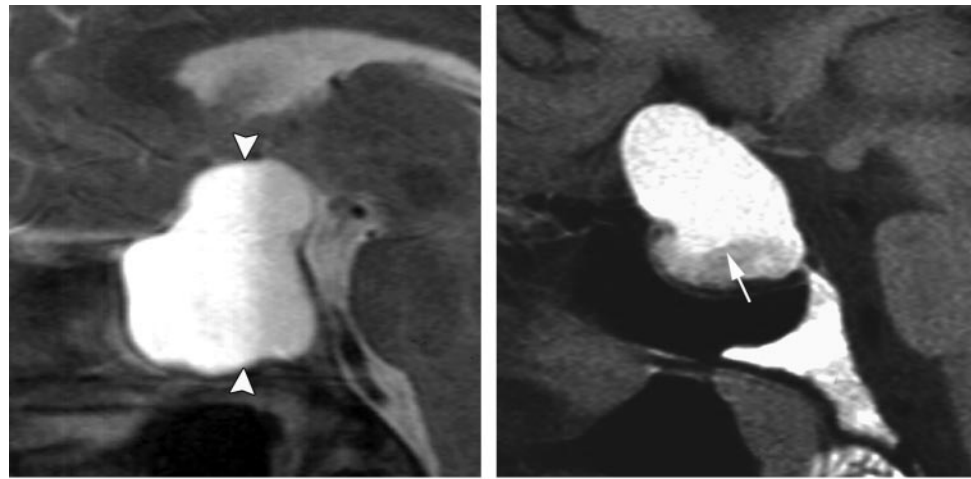


**Figure 19.** Hemorrhagic pituitary macroadenoma (**a**) and craniopharyngioma (**b**). At an initial comparison of the sagittal T2-weighted image (**a**) and the T1-weighted image (**b**), these two different lesions may appear to have similar features: a sellar-suprasellar location, enlargement of the sella turcica, and mixed signal intensities. However, the distinctive hemorrhagic fluid-debris level visible on **a** (arrowheads) is more frequently observed in macroadenomas than in craniopharyngiomas, in which a proteinaceous pseudo-fluid-fluid level (arrow in **b**) may be depicted.

calcified, and cystic components (33). The cystic component may contain a high concentration of protein and have a high signal intensity on T1-weighted images (Fig 18). It is not always easy to distinguish between a craniopharyngioma and a hemorrhagic pituitary macroadenoma, and, in some cases, the imaging appearance may not be definitive. **The fluid-fluid level is more likely to be observed in hemorrhagic adenomas than in craniopharyngiomas, in which only a pseudo-fluid-fluid level may be seen** that corresponds to tenacious secretions or to a fortuitous position of the interface between the fluid and solid components of the tumor (Fig 19).

#### Teaching Point

**Mucocèles and Cholesterol Granulomas.**—Mucocèles and cholesterol granulomas of the sphenoid sinus are rare (34). Both types of lesion result from a chronic obstruction of the sinus that leads to the accumulation and dehydration of secretions and of their protein contents. The increase in local protein concentration results in T1 shortening. Mucocèles thus appear as expansive well-delineated masses with a homogeneously hyperintense T1 and T2 signal. In cholesterol granulomas, chronic inflammation of the mucosa leads to microvascular hemorrhage and increased

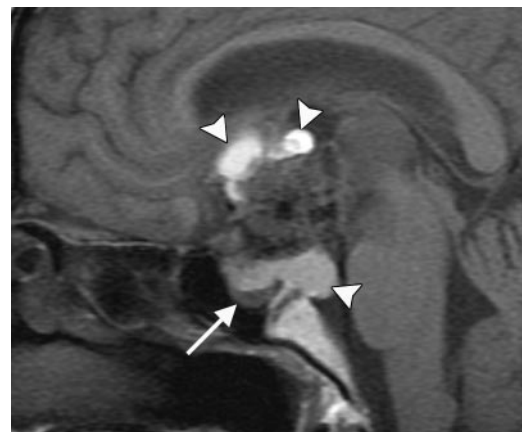


**Figure 18.** Recurrent craniopharyngioma in a 23-year-old man with visual impairment and diabetes insipidus. Sagittal T1-weighted image depicts an enormous heterogeneous suprasellar lesion with hyperintense cystic components (arrowheads), findings that are consistent with high concentrations of protein. Note the normal pituitary gland (arrow) beneath the lesion.

accumulation of blood breakdown products such as cholesterol crystals, which trigger a foreign-body reaction (35). The MR appearance of cholesterol granulomas is very similar to that of mucocèles, except for a thin peripheral rim of low signal intensity suggestive of cortical bone protuberance and/or the presence of hemosiderin (Fig 20) (36).



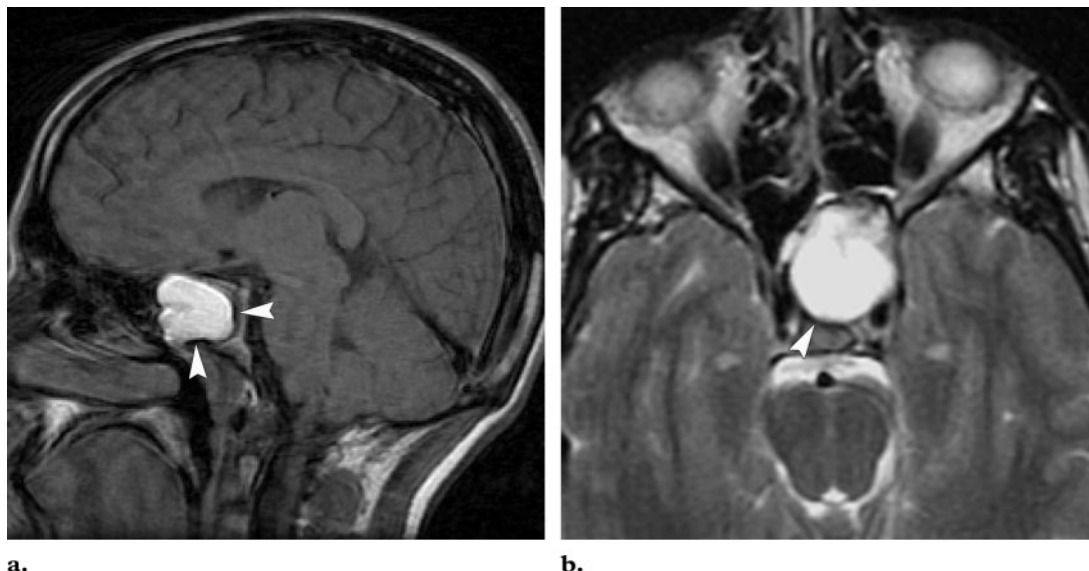


**Figure 20.** Cholesterol granuloma of the sphenoid sinus in a 45-year-old woman with headache. **(a)** Sagittal T1-weighted image shows a homogeneous hyperintense infrasellar lesion that has filled the sphenoid sinus and displaced the pituitary gland upward. **(b)** Axial T2-weighted image shows high signal intensity in the lesion. The thin rim of signal hypointensity (arrowheads) visible on both images suggests the diagnosis. (Courtesy of Gul Moonis, MD.)

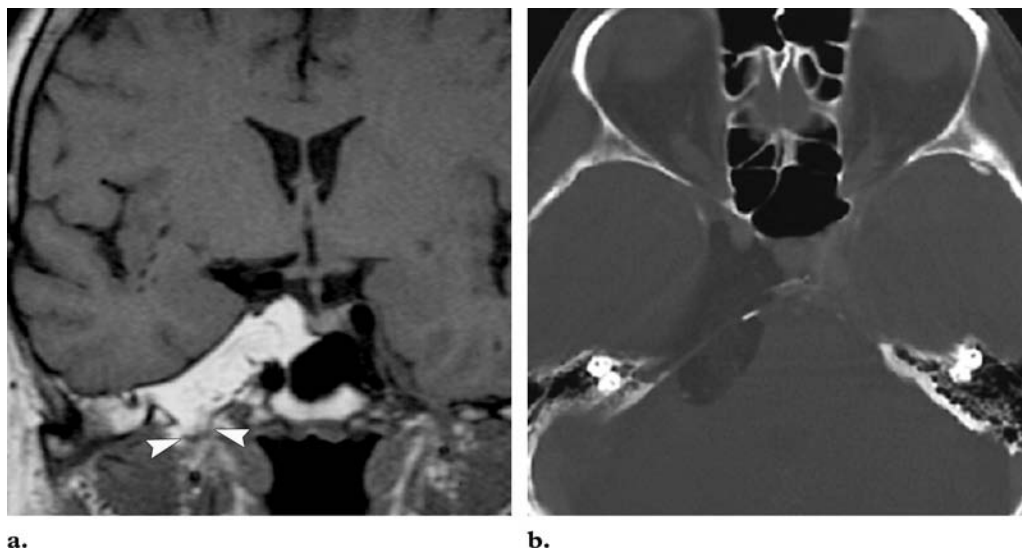


**Figure 21.** Trigeminal lipoma in a 34-year-old woman with right-sided facial neuralgia. **(a)** Coronal T1-weighted image depicts a right laterosellar hyperintense lesion that occupies the posterior aspect of the cavernous sinus and emerges through the foramen ovale (arrowheads). **(b)** Axial CT scan demonstrates the pure fatty nature of the lesion, which parallels the trigeminal nerve and its branches.

### Lesions with High Fat Content

Only a few types of intracranial tumors contain a substantial fatty component. In the sellar area, they are essentially limited to lipomas and dermoid cysts, which have the signal intensity characteristics of fat (eg, high signal intensity on T1-weighted images, low signal intensity on images obtained with fat suppression).

**Lipomas.**—Lipomas are benign lesions that are commonly believed to result from a maldifferentiation of the primitive meninx (37). In the sellar area, they occur as extraaxial lesions that adhere to the floor of the third ventricle, the infundibulum, or the adjacent cranial nerves (Fig 21). Most

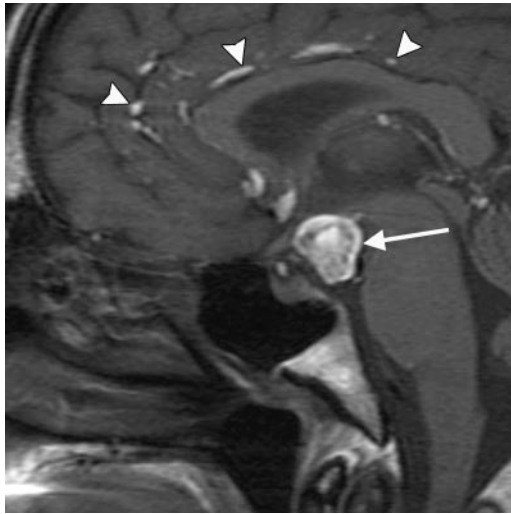


**Figure 22.** Ruptured dermoid cyst in a 50-year-old man with sudden headache. Sagittal T1-weighted image depicts a large heterogeneously hyperintense suprasellar dermoid cyst (arrow) and multiple subarachnoid foci of high signal intensity consistent with fat accumulations (arrowheads).

lipomas are asymptomatic, but very large lipomas may compress normal structures and produce symptoms. At imaging, lipomas demonstrate signal intensity equal to that of subcutaneous fat on MR images, are usually homogeneous (except for possible superficial calcification, which is best seen on CT images), and show no enhancement after contrast medium administration.

**Dermoid Cysts.**—Dermoid cysts are congenital inclusion cysts that appear as well-circumscribed heterogeneous extraaxial masses. Their contents may vary and may include, for example, fat and calcifications or teeth. The sellar or parasellar region is the most frequent site of their occurrence. Dermoid cysts may rupture in the subarachnoid space, causing aseptic meningitis and producing the nearly pathognomonic MR appearance of T1-hyperintense speckles in the cortical sulci and a fat-fluid level in the ventricles (Fig 22) (38).

However, multiple small hyperintense subarachnoid foci also could represent remnants of iodinated lipid-containing contrast material retained in the chiasmatic cistern (Fig 23) (39).

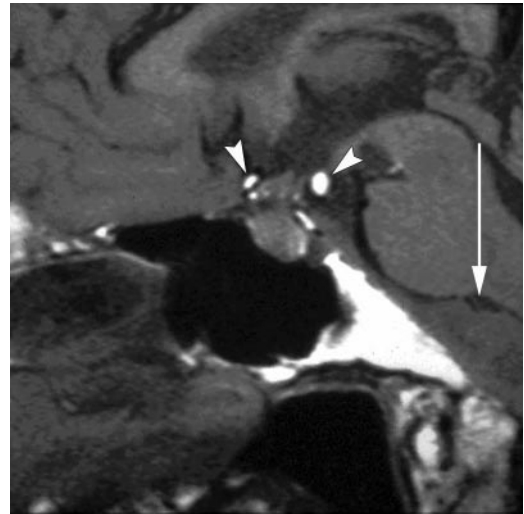


**Figure 23.** Subarachnoid remnants of contrast material in a 72-year-old woman with a history of intrathecal injection of an iodinated lipid-containing contrast agent for better visualization of a meningeoma (arrow) in the foramen magnum. Sagittal T1-weighted image shows multiple hyperintense nodules trapped in the chiasmatic cistern (arrowheads).

Therefore, a past history of an intrathecal injection of such an agent should be sought in the presence of multiple spots of high T1 signal intensity in the subarachnoid spaces. Because of the iodine content, retained droplets of such contrast materials have higher attenuation on CT scans than do ruptured dermoid cysts.

**Meningiomas.**—Another rare fat-containing tumor that may occur in the sellar area is so-called lipomatous meningioma. This extraaxial tumor has the same shape as other meningiomas but contains lipid-laden meningotheial cells (which account for 10%–90% of its contents) and other cells that resemble mature adipocytes (Fig 24) (40).

### Calcifications

Intratumoral calcification is best depicted with CT and usually has no signal on spin-echo MR images. However, the degree of attenuation in calcified tissue at CT and the signal pattern at MR imaging depend on the degree of mineralization, and calcification should be considered when foci of mild T1 signal hyperintensity are observed in a lesion at MR imaging and then are confirmed

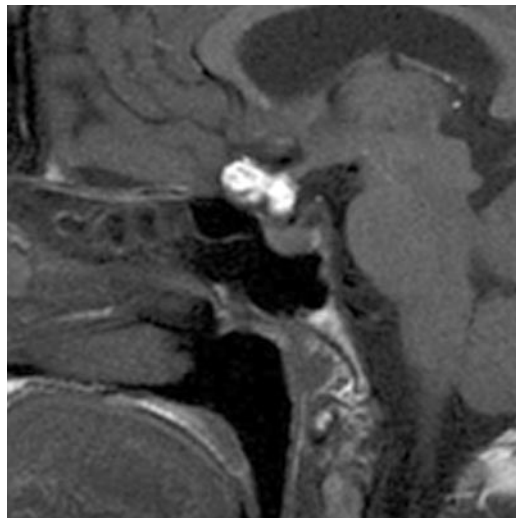
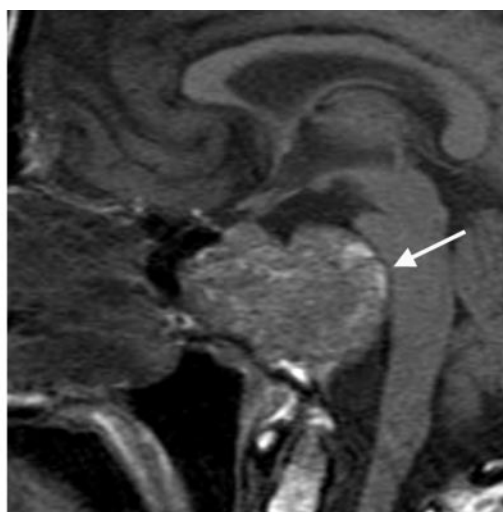


**Figure 24.** Lipomatous meningioma in the tuberculum sellae in a 29-year-old woman with mild hyperprolactinemia. Sagittal unenhanced T1-weighted image depicts an extraaxial suprasellar mass with high signal intensity, in the same location and with the same shape as other commonly observed meningiomas but with an atypical, fat signal intensity. (Courtesy of Jean-Luc Sarrazin, MD.)



**a.**



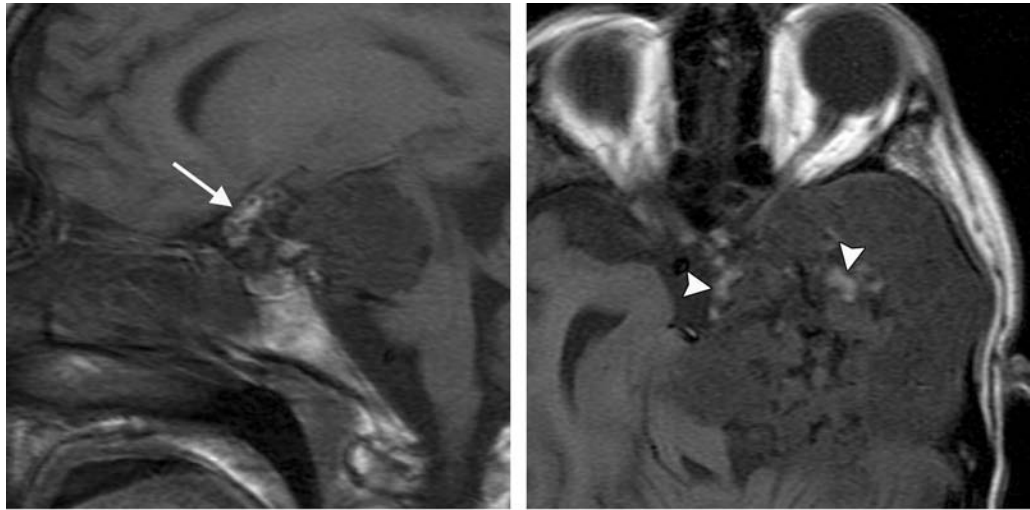
**b.**

**Figure 25.** Chordoma in a 73-year-old man. **(a)** Unenhanced CT scan shows, midline, a destructive mass of the clivus, with posterior peripheral calcification and with a fluid-fluid level in a hemorrhagic cystic component (arrow). **(b)** Sagittal T1-weighted image depicts a heterogeneous chordoma that impinges on the pons (arrow) and that contains high-signal-intensity foci with various origins. Note the typical speckled pattern of mixed isointense and hyperintense signals.

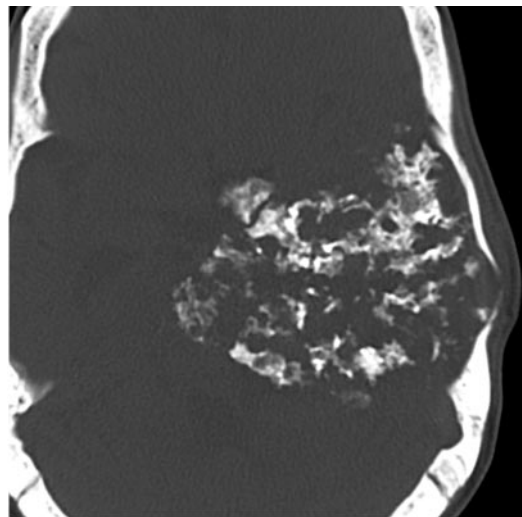
at CT (41). It is of fundamental importance to detect calcification in a sellar lesion, because the finding helps restrict the differential diagnosis to craniopharyngioma, aneurysm, chordoma, and cartilaginous tumor.

**Chordomas.**—Chordomas are neoplasms that derive from remnants of the notochord. Intracranial chordomas arise mainly from the clivus and are locally invasive and destructive. The infrasellar midline masses usually have T1 signal hypoin-

tensity and T2 signal hyperintensity, with suggestive hypointense intratumoral septations and posterior extension indenting the pons (42). However, foci of T1 signal hyperintensity also may be depicted within the tumor or at its periphery, findings that may represent residual ossified fragments, tumor calcifications, small collections of proteinaceous fluid, or hemorrhage (Fig 25).



**a.**  
**Figure 26.** Chondrosarcoma in a 37-year-old man with intracranial hypertension. **(a)** Sagittal T1-weighted image depicts a suprasellar lesion with high signal intensity at its anterior aspect (arrow). **(b)** Axial T1-weighted image shows more foci of high signal intensity (arrowheads), as well as areas of low signal intensity, and shows that the lesion center is not at the midline. **(c)** CT scan shows massive calcification, a finding that is highly suggestive of a chondromatous tumor.



**c.**

**Cartilaginous Tumors.**—Cartilaginous tumors (chondroma and chondrosarcoma) may mimic chordomas, but they usually have a more lateral location, farther from the midline, at the petrooccipital synchondrosis (43). The typical chondroid calcifications are curvilinear and have low signal intensity on MR images acquired with spin-echo sequences. However, they also may appear as areas of hyperintense signal on T1-weighted images, depending on the degree of mineralization (Fig 26).

### Other Lesions

**Abscesses.**—Pituitary abscesses are very rare. They may occur in isolation, in association with a local and/or regional intracranial infection, or in systemic sepsis in an immunocompromised patient. They usually appear as intrasellar lesions with characteristic rim enhancement and associated adjacent inflammatory reaction (44). Hyperintense signal may be observed either at the periphery of the lesion or within it. Indeed, an intrinsically hyperintense rim like that in brain

abscesses may be seen in the capsule of the lesion on T1-weighted images. This finding may reflect paramagnetic T1 shortening due to the presence of free radicals, the products of phagocytosis by macrophages (Fig 27) (45). On the other hand, high T1 signal intensity observed in the center of an abscess may correspond to a small amount of blood breakdown products in the proteinaceous purulent contents of the abscess (46).

**Excess Manganese.**—Liver disease and parenteral nutrition are two major conditions in which an excess of circulating manganese exists. For unknown reasons, the excess may accumulate in the anterior pituitary lobe and globus pallidus (Fig 28) (47). Therefore, the association of homogeneous T1 signal hyperintensity of the adenohypophysis and globus pallidus bilaterally is a



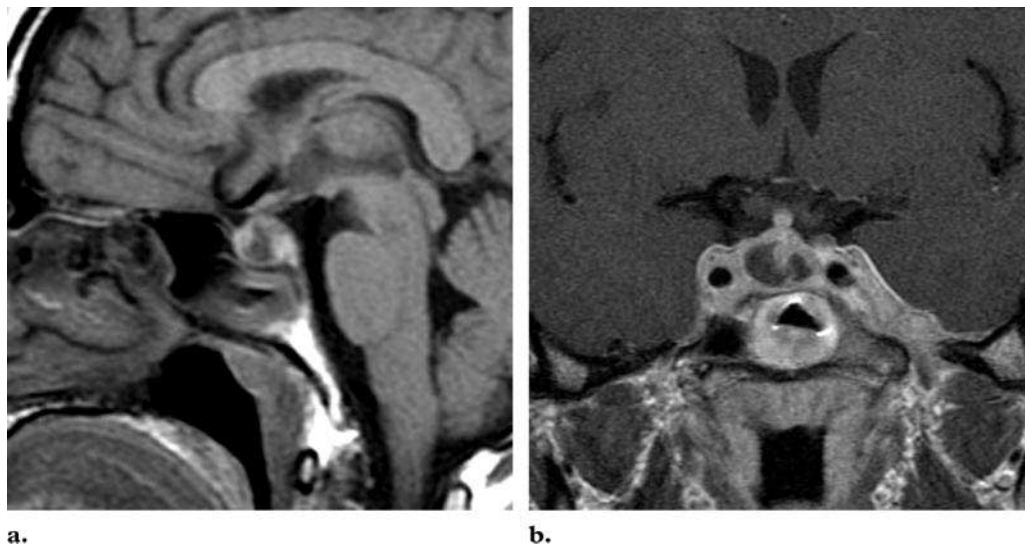


**Figure 27.** Pituitary abscess in a 28-year-old man with febrile cephalalgia. **(a)** Sagittal T1-weighted image depicts a heterogeneous intrasellar lesion with a hyperintense peripheral capsule. **(b)** Contrast-enhanced coronal T1-weighted image shows gadolinium uptake characteristic of a pituitary abscess, a finding that extends to the adjacent cavernous sinuses and left temporal dura mater.

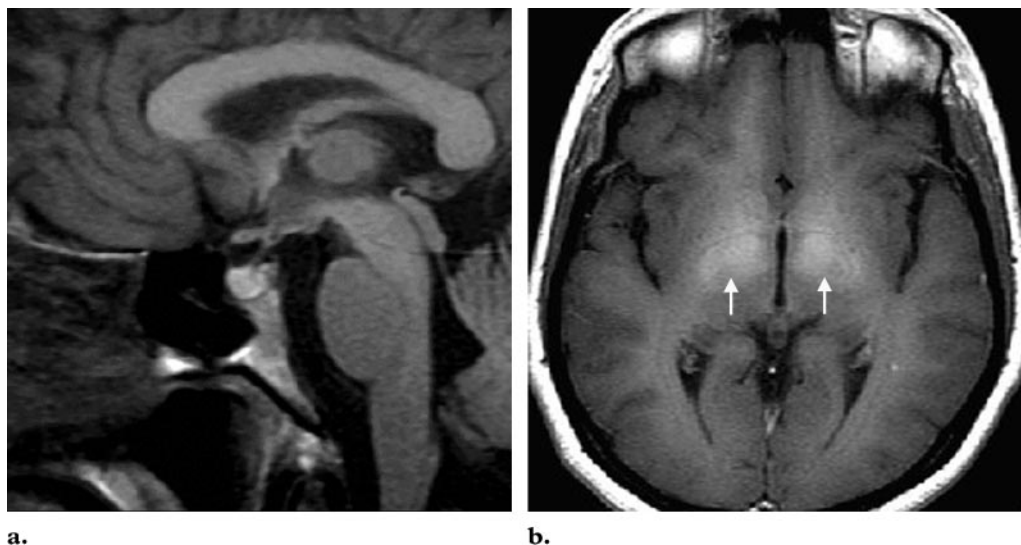


**Figure 28.** Hypermanganesemia in a 32-year-old woman receiving intravenous nutrition in an intensive care unit. Sagittal **(a)** and axial **(b)** T1-weighted images show homogeneously hyperintense signal in the anterior pituitary lobe and the globus pallidus (arrows), a finding suggestive of this condition.

common pattern at cerebral MR imaging in patients receiving parenteral nutrition in an intensive-care unit, or in patients with chronic liver deficiency.

**Melanomas.**—Primitive or metastatic melanin tumors are very uncommon in the sella, but they may occur (48). The melanin contained in these

lesions is a paramagnetic substance that has a T1-shortening effect and is therefore a source of spontaneous T1 signal hyperintensity and T2 signal hypointensity. Although the lesions may be hemorrhagic, the signal pattern correlates best with the paramagnetic properties of melanin.



**Figure 29.** Fat packing in the postoperative bed of a pituitary adenoma. Coronal T1-weighted image obtained 3 months after surgery shows a homogeneous hyperintense berrylike region of fatty material, with a characteristic dark outline that represents a chemical shift artifact (arrowheads).

### Posttherapeutic Conditions

Various posttherapeutic conditions may arise as a result of surgery or medical treatment and may cause high T1 signal intensity.

#### Postoperative Conditions

**Blood Products.**—Blood breakdown products are normally seen in the lesion bed at early postoperative follow-up MR imaging of patients with pituitary tumors, even if there is no clinical evidence of hemorrhagic complications. Of course, if a tear of a cavernous sinus or injury to an internal carotid artery occurs during surgery, a more dramatic appearance of hemorrhage will be present.

**Surgical Packing Materials.**—After excision of a sellar lesion with a transsphenoidal approach, neurosurgeons may pack the operative bed to stop a cerebrospinal fluid leak or hemorrhage. Fat may be taken from the thigh and placed within the sella and the sphenoid sinus if a cerebrospinal fluid leak is recognized during surgery (49). The classic MR imaging appearance of the subcutaneous fat is that of an area of homogeneous hyperintense T1 signal outlined by a chemical shift artifact (Fig 29). The fat pad is slowly resorbed but may remain visible at MR imaging for several years after the surgical procedure (19,49).

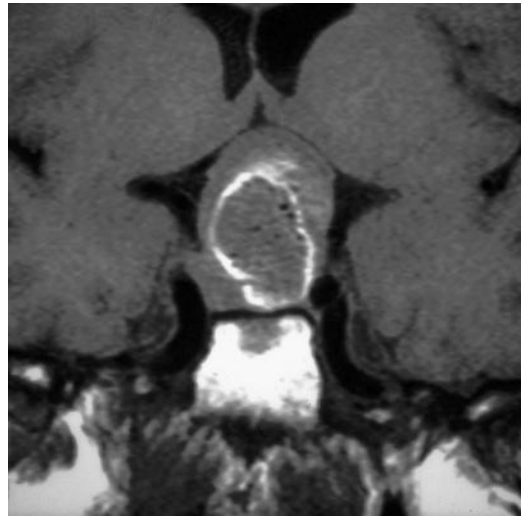
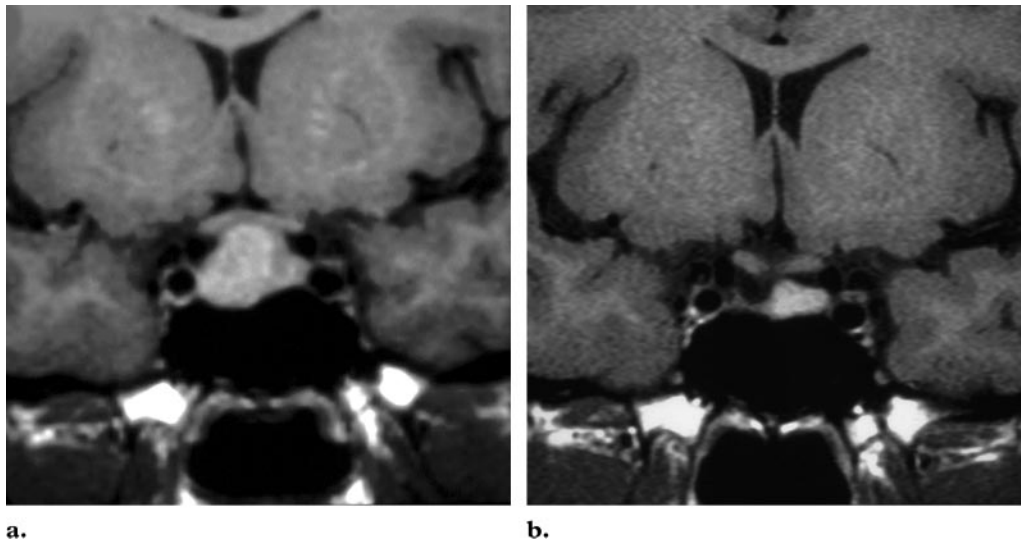


**Figure 30.** Blood-impregnated gelatin sponge. Coronal T1-weighted image acquired 1 week after surgical excision of a pituitary macroadenoma shows specific MR features that include a thin peripheral rim of high signal intensity, which corresponds to methemoglobin, and scattered spots of signal void, which correspond to bubbles of air trapped in the gelatin sponge.



**Figure 31.** Metal artifact in the postoperative bed of a macroadenoma. Sagittal T1-weighted image obtained 4 days after surgery shows metallic artifacts along the transsphenoidal path of approach, which appear as areas of no signal, with peripheral hyperintense dots (arrowheads). Note that the space left by the adenoma has not yet decreased at early follow-up MR imaging.

In case of hemorrhage, gelatin sponge may be left in place for local hemostasis. Gelatin sponge that is impregnated with blood has a pathognomonic MR imaging pattern during the first few weeks following surgery: The center shows isointense T1 signal, with scattered trapped small air



**a.** **b.**  
**Figure 32.** Hyperactivity of residual normal pituitary gland after medical treatment of a prolactin-secreting macroadenoma in a 19-year-old woman with primary amenorrhea. Coronal T1-weighted images before (**a**) and 18 months after (**b**) therapy with oral bromocriptine for normalization of prolactinemia and menstruation show the complete posttreatment disappearance of the lesion in the right aspect of the sella. In addition, the signal intensity in the residual normal pituitary tissue in the left aspect of the sella has increased to a level exceeding that in the white matter of the temporal lobes.

bubbles in which there is no signal, whereas a rim of T1 hyperintensity, which represents methemoglobin, is seen at the periphery of the embolic material (Fig 30) (19,49). Gelatin sponge is resorbed more quickly than fat and usually has vanished in less than 1 year.

An excess of embolic material also may result in T1 signal hyperintensity of the sellar and parasellar region. Indeed, it might lead to intrasellar hypertension and local venous engorgement or place direct pressure on the medial veins of the cavernous sinuses. Both mechanisms would cause a reduction of flow in the veins, with resultant T1 signal hyperintensity.

**Metallic Artifacts.**—During surgical access with a transsphenoidal approach to a tumor or aneurysm, drilling of the sphenoid bone may be required. The procedure sometimes causes tiny bits of metallic debris to separate from the surgical tools. These metallic particles, which are not visible on plain radiographs, are easily detected on MR images because they create heterogeneity of the magnetic field and, therefore, an artifact. Metallic artifacts have very specific and easily recognizable features on all MR images. On T1-weighted images, a complete lack of signal in the center and a thin peripheral rim of hyperintense signal are observed (Fig 31) (22).

**Mucocele.**—During surgery with a transsphenoidal approach, access is achieved through the sphenoid sinus. A potential complication of this approach is therefore the obstruction of the sphenoid sinus by scar tissue, which may lead to the accumulation of mucous secretions and, thus, a mucocele (50). The postoperative lesion has the same MR imaging features as the previously described classic postinflammatory mucocele.

### Conditions Caused by Medical Therapy

**Hemorrhage.**—Bromocriptine has been reported to induce intratumoral hemorrhage without any adverse clinical effects (51). This phenomenon appears the same as any other hemorrhagic event in a pituitary adenoma at MR imaging. T1 signal hyperintensity related to the presence of methemoglobin therefore could appear on follow-up MR images of pituitary adenomas that previously appeared isointense at MR imaging.

**Hyperactivity of Residual Adenohypophysis.**—Homogeneous T1 signal hyperintensity of the normal pituitary gland itself has been described after medical cure of pituitary adenomas (Fig 32)

(52). Indeed, when only a low volume of normal residual adenohypophysis remains after medical (or surgical) treatment of a pituitary adenoma, hyperactivity of the residual functioning gland may be needed to maintain pituitary hormonal levels within normal ranges. Hypersecretion of hormones at the cellular level causes a subtle homogeneous T1 signal hyperintensity in the pituitary remnant.

### Conclusions

T1 signal hyperintensity of various degrees is observed at MR imaging of the sellar region. Vasopressin storage, bone marrow, and adenohypophysial hyperactivity are the three main causes of high T1 signal intensity in normal conditions. Lesions that contain blood products, fat, high concentrations of protein, or calcifications account for the majority of pathologic entities that cause high T1 signal intensity in the sellar and parasellar regions. Embolic materials (eg, gelatin sponge) and blood are the usual sources of T1 signal hyperintensity on images obtained after medical or surgical treatment of a sellar lesion.

**Acknowledgments:** The authors are grateful to David Seidenwurm, MD, for his valuable review of the manuscript and to Gilles Podevins for the preparation of images.

### References

1. Mark L, Pech P, Daniels D, Charles C, Williams A, Haughton V. The pituitary fossa: a correlative anatomic and MR study. *Radiology* 1984;153:453-457.
2. Fujisawa I, Asato R, Nishimura K, et al. Anterior and posterior lobes of the pituitary gland: assessment by 1.5 T MR imaging. *J Comput Assist Tomogr* 1987;11:214-220.
3. Fujisawa I, Nishimura K, Asato R, et al. Posterior lobe of the pituitary in diabetes insipidus: MR findings. *J Comput Assist Tomogr* 1987;11:221-225.
4. Fujisawa I, Asato R, Kawata M, et al. Hyperintense signal of the posterior pituitary on T1-weighted MR images: an experimental study. *J Comput Assist Tomogr* 1989;13:371-377.
5. Kucharczyk J, Kucharczyk W, Berry I, et al. Histological characterization and functional significance of the hyperintense signal on MR images of the posterior pituitary. *AJR Am J Roentgenol* 1989;152:153-157.
6. Kucharczyk W, Lenkinski RE, Kucharczyk J, Henkelman RM. The effect of phospholipid vesicles on the NMR relaxation of water: an explanation for the MR appearance of the neurohypophysis? *AJNR Am J Neuroradiol* 1990;11:693-700.
7. Elster AD. Modern imaging of the pituitary. *Radiology* 1993;187:1-14.
8. Kurokawa H, Fujisawa I, Nakano Y, et al. Posterior lobe of the pituitary gland: correlation between signal intensity on T1-weighted MR images and vasopressin concentration. *Radiology* 1998;207:79-83.
9. Cattin F, Bonneville J. Imagerie normale de la région hypothalamohypophysaire. In: *Encyclopédie médico-chirurgicale. Radiodiagnostic—squelette normal*. Paris, France: Elsevier, 1998; 30-810-A-20.
10. Fujisawa I, Asato R. MR imaging findings in the posterior pituitary gland. *Radiology* 1988;168:282-283.
11. Colombo N, Berry I, Kucharczyk J, et al. Posterior pituitary gland: appearance on MR images in normal and pathologic states. *Radiology* 1987;165:481-485.
12. Fujisawa I, Kikuchi K, Nishimura K, et al. Transection of the pituitary stalk: development of an ectopic posterior lobe assessed with MR imaging. *Radiology* 1987;165:487-489.
13. Kuroiwa T, Okabe Y, Hasuo K, Yasumori K, Mizushima A, Masuda K. MR imaging of pituitary dwarfism. *AJNR Am J Neuroradiol* 1991;12:161-164.
14. Bonneville F, Narboux Y, Cattin F, Rodière E, Jacquet G, Bonneville J. Preoperative location of the pituitary bright spot in patients with pituitary macroadenomas. *AJNR Am J Neuroradiol* 2002;23:528-532.
15. Cox TD, Elster AD. Normal pituitary gland: change in shape, size, and signal intensity during 1st year of life at MR imaging. *Radiology* 1991;179:721-724.
16. Elster AD, Sanders TG, Vines FS, Chen MY. Size and shape of the pituitary gland during pregnancy and post partum: measurement with MR imaging. *Radiology* 1991;181:531-535.
17. Miki Y, Asato R, Okumura R, et al. Anterior pituitary gland in pregnancy: hyperintensity at MR. *Radiology* 1993;187:229-231.
18. Madeline L, Elster A. Suture closure in the human chondrocranium: CT assessment. *Radiology* 1995;196:747-756.
19. Bonneville JF, Bonneville F, Schillo F, Cattin F, Jacquet G. Follow-up MRI after trans-sphenoidal surgery [in French]. *J Neuroradiol* 2003;30:268-279.
20. Dietemann JL, Lang J, Francke JP, Bonneville JF, Clarisse J, Wackenheim A. Anatomy and radiology of the sellar spine. *Neuroradiology* 1981;21:5-7.
21. Abs R, Van Breusegem L, Verhaert G, Smet H, Parizel P. Intraseellar bony spine, a possible cause of hypopituitarism. *Eur J Endocrinol* 1995;132:82-85.



22. Kastler B, Vetter D, Patay Z. Artéfacts en IRM. In: Kastler B, ed. *Comprendre l'IRM*. 2nd ed. Paris, France: Masson, 1997; 161–184.
23. Mohr G, Hardy J. Hemorrhage, necrosis, and apoplexy in pituitary adenomas. *Surg Neurol* 1982; 18:181–189.
24. Ostrov SG, Quencer RM, Hoffman JC, Davis PC, Hasso AN, David NJ. Hemorrhage within pituitary adenomas: how often associated with pituitary apoplexy syndrome? *AJR Am J Roentgenol* 1989;153:153–160.
25. Piotin M, Tampieri D, Rufenacht D, et al. The various MRI patterns of pituitary apoplexy. *Eur Radiol* 1999;9:918–923.
26. Rogg JM, Tung GA, Anderson G, Cortez S. Pituitary apoplexy: early detection with diffusion-weighted MR imaging. *AJNR Am J Neuroradiol* 2002;23:1240–1245.
27. Atlas SW, DuBois P, Singer MB, Lu D. Diffusion measurements in intracranial hematomas: implications for MR imaging of acute stroke. *AJNR Am J Neuroradiol* 2000;21:1190–1194.
28. Bonneville F, Cattin F, Bonneville J, et al. Rathke's cleft cyst [in French]. *J Neuroradiol* 2003;30:238–248.
29. Arita K, Kurisu K, Tominaga A, et al. Thickening of sphenoid sinus mucosa during the acute stage of pituitary apoplexy. *J Neurosurg* 2001;95:897–901.
30. Dejager S, Gerber S, Foubert L, Turpin G. Sheehan's syndrome: differential diagnosis in the acute phase. *J Intern Med* 1998;244:261–266.
31. Hayashi Y, Tachibana O, Muramatsu N, et al. Rathke cleft cyst: MR and biomedical analysis of cyst content. *J Comput Assist Tomogr* 1999;23: 34–38.
32. Byun W, Kim O, Kim D. MR imaging findings of Rathke's cleft cysts: significance of intracystic nodules. *AJNR Am J Neuroradiol* 2000;21:485–488.
33. Pusey E, Kortman KE, Flannigan BD, Tsuruda J, Bradley WG. MR of craniopharyngiomas: tumor delineation and characterization. *AJR Am J Roentgenol* 1987;149:383–388.
34. Yonezawa K, Shirataki K, Sakagami Y, Kohmura E. Panhypopituitarism induced by cholesterol granuloma in the sellar region: case report. *Neurol Med Chir (Tokyo)* 2003;43:259–262.
35. Pellet W, Valenzuela S, Malca S, Cannoni M, Perez-Castillo A. Giant cholesterol cysts of the petrous apex [in French]. *Neurochirurgie* 1992; 38:267–280.
36. Bonneville F, Barrali E, Cattin F, Viennet G, Czorny A, Bonneville J. What is your diagnosis? cholesterol granuloma [in French]. *J Neuroradiol* 1999;26:147–149.
37. Guy G, Alhayek G, Menei P, Mercier P. Tumeurs congénitales non neuroépithéliales. In: *Encyclopédie médico-chirurgicale. Neurologie*. Paris, France: Elsevier, 1993; 17–260-C-10.
38. Smirniotopoulos JG, Chiechi MV. Teratomas, dermoids, epidermoids of the head and neck. *RadioGraphics* 1995;15:1437–1455.
39. Braun IF, Malko JA, Davis PC, Hoffman JC Jr, Jacobs LH. The behavior of Pantopaque on MR: in vivo and in vitro analysis. *AJNR Am J Neuroradiol* 1986;7:997–1001.
40. Withers T, Klevansky A, Weinstein S. Lipomeningioma: case report and review of the literature. *J Clin Neurosci* 2003;10:712–714.
41. de Kerviler E, Cuenod C, Clement O, Halimi P, Frija G, Frija J. What is bright on T1 MRI scans? [in French]. *J Radiol* 1998;79:117–126.
42. Erdem E, Angtuaco E, Van Hemert R, Park J, Al-Mefty O. Comprehensive review of intracranial chordoma. *RadioGraphics* 2003;23: 995–1009.
43. Bonneville F, Sarrazin JL, Marsot-Dupuch K, et al. Unusual lesions of the cerebellopontine angle: a segmental approach. *RadioGraphics* 2001;21: 419–438.
44. Takahashi T, Shibata S, Ito K, Ito S, Tanaka M, Suzuki S. Neuroimaging appearance of pituitary abscess complicated with close inflammatory lesions: case report. *Neurol Med Chir (Tokyo)* 1998;38:51–54.
45. Haimes A, Zimmerman R, Morgello S, et al. MR imaging of brain abscesses. *AJR Am J Roentgenol* 1989;152:1073–1085.
46. Abs R, Parizel P, Verlooy J, Neetens I, Arnouts P. MR characterization of a long-standing pituitary abscess. *J Endocrinol Invest* 1993;16:635–637.
47. Diniz RL, Reimund JM, Duclos B, Reis M Jr, Baumann R, Dietemann JL. Hyperintensité spontanée de l'antéhypophyse en séquence pondérée T1 par dépôts de manganèse chez un patient sous nutrition parentérale prolongée. *J Radiol* 1998;79: 345–347.
48. Chappell PM, Kelly WM, Ercius M. Primary sellar melanoma simulating hemorrhagic pituitary adenoma: MR and pathologic findings. *AJNR Am J Neuroradiol* 1990;11:1054–1056.
49. Dina TS, Feaster SH, Laws ER Jr, Davis DO. MR of the pituitary gland postsurgery: serial MR studies following transsphenoidal resection. *AJNR Am J Neuroradiol* 1993;14:763–769.
50. Buchinsky FJ, Gennarelli TA, Strome SE, Deschler DG, Hayden RE. Sphenoid sinus mucocoele: a rare complication of transsphenoidal hypophysectomy. *Ear Nose Throat J* 2001;80: 886–888.
51. Yousem DM, Arrington JA, Zinreich SJ, Kumar AJ, Bryan RN. Pituitary adenomas: possible role of bromocriptine in intratumoral hemorrhage. *Radiology* 1989;170:239–243.
52. Bonneville F, Cattin F, Barrali E, Lucas X, Narboux Y, Bonneville J. Hypersignal T1 de l'antéhypophyse saine résiduelle après traitement médical des adénomes à prolactine. *J Radiol* 2001; 82:501–505.

## Teaching Points for T1 Signal Hyperintensity in the Sellar Region: Spectrum of Findings

*Fabrice Bonneville, MD, et al*

RadioGraphics 2006; 26:93–113 • Published online 10.1148/rg.261055045 • Content Codes: MR NR

---

### Page 95

The resultant focal spot of high signal intensity on MR images correlates with normal function and is observed where the vasopressin is stored, normally in the posterior pituitary lobe. A focus of high signal intensity also may be observed outside the sella in individuals in whom the hypothalamohypophysial axis is interrupted or extrinsically compressed.

### Page 96

Various normal physiologic circumstances may produce anterior pituitary lobe hyperactivity in the form of cellular hormonal hypersecretion, which results in an increase in the intracellular protein concentration and, therefore, a shortening of T1. These circumstances include the first few weeks of life for newborns (Fig 3) and, for women, pregnancy, the postpartum period, and lactation.

### Page 100

Early in the course of pituitary apoplexy, MR images depict a mass lesion that has heterogeneous signal intensity, with predominant hyperintensity on T1 images and predominant hypointensity on T2-weighted images. Thickening of the mucosa of the sphenoid sinus is an MR feature suggestive of the early hours of pituitary apoplexy.

### Page 102

Thus, typical Rathke cleft cysts appear as nonenhancing well-demarcated intrasellar rounded lesions located exactly at the midline between the anterior and posterior pituitary lobes. The cysts have a homogeneously hyperintense T1 signal and, often, a hypointense T2 signal.

### Page 104

The fluid-fluid level is more likely to be observed in hemorrhagic adenomas than in craniopharyngiomas, in which only a pseudo-fluid-fluid level may be seen.

E210



# RadioGraphics

## Errata

November-December 2021 • Volume 41 • Number 7

---

**Originally published in:**

RadioGraphics 2006; 26(1):93–113 • <https://doi.org/10.1148/rg.261055045>

T1 Signal Hyperintensity in the Sellar Region: Spectrum of Findings

Fabrice Bonneville, Françoise Cattin, Kathlyn Marsot-Dupuch, Didier Dormont, Jean-François Bonneville, Jacques Chiras

**Erratum in:**

RadioGraphics 2021; 41(7):E210 • <https://doi.org/10.1148/rg.2021219011>

**Page 109, Figure 28:** The legend for Figure 28 should read as follows: **Hypermanganesemia** in a 32-year-old woman receiving intravenous nutrition in an intensive care unit. Sagittal (a) and axial (b) T1-weighted images show homogeneously hyperintense signal in the anterior pituitary lobe and the globus pallidus (arrows), a finding suggestive of this condition.